Quantum Electronics **47** (4) 335–342 (2017)

HOLOGRAPHIC MEMORY

https://doi.org/10.1070/QEL16310

Detection of common fragments in a series of images by superimposed volume Fourier holograms

A.V. Pavlov

Abstract. **The paper adresses the problem of detecting common fragments in a sequence of images recorded in volume recording medium by the method of superimposed Fourier holograms in the joint-transform scheme. As applied to the description of images as realisations of a homogeneous random field, the dependence of the detection efficiency on the number of superimposed holograms is analysed by estimating the image information capacity and the common and distinct fragments of images in the recorded sequences. Theoretical conclusions are confirmed by the results of numerical experiments.**

Keywords: *superimposed holograms, multiplex hologram, volume recording medium, holographic memory, Fourier hologram, data processing, correlation, image series, detection of common fragments.*

1. Introduction

Systems of holographic memory conventionally utilise the technology of superimposed holograms (SHs), that is, holograms that are recorded to the same domain of a holographic recording medium (HRM) [1–7]. To this end, a working (conventionally quasi-linear) part of the dynamic range of the HRM exposure characteristic is divided into subranges for recording one hologram into each of them. The set of holograms recorded to a particular HRM domain constitutes a multiplex hologram.

The SH method is mainly used for increasing memory capacity [1–4] and performance [5–7]. The main approach refers to a volume HRM. This substantially increases the density of stored data due to the angular selectivity of volume holograms; however, the shift invariance is lost in this case.

In addition to memory as such, the SH method is actual for realising memory-based models of processing the data presented by time or spatial sequences [8–12], including search for regular properties and revealing cause-and-effect relations in a chain of events [13]. In this context, the key item in solving such problems is to reveal common, that is, completely correlated fragments in a sequence of images. This is important, for example, for analysing real-time stream video data [14].

One possible approach to solving the problem by the SH Fourier method was suggested and preliminarily simulated in [15]. The approach was developed in our paper [16], where we analysed the dependence of the efficiency of revealing correlated fragments on the image information capacity and the conditions of hologram recording while describing images as realisations of homogeneous random fields. However, the analysis in [16] was only performed for the simplest case, namely, the case of completely orthogonal distinct fragments of reference images under the assumption that the Fourier transformation invariance to shifts is not preserved. Theoretical conclusions were illustrated by the results of numerical experiments on examples of processing realisations of stationary random processes.

However, real images are characterised by a partial correlation rather than by orthogonality. For excluding crosstalk in dealing with partially correlated reference and signal images, additional methods are used, such as the phase coding by orthogonal masks [17]. Nevertheless, the orthogonalisation methods for processed images cannot be employed in the considered problem of revealing common fragments, because the orthogonalisation breaks correlation of not only background but also of searched common fragments. Hence, it is topical to analyse the dependence of the efficiency of revealing common fragments in the image on the number of SHs and the HRM characteristics in a more general and realistic case of a partial correlation between distinct fragments of image than in [16].

Developing works [15, 16], we consider the Fourier holographic scheme with volume hologram recording by the joint transformation scheme. A more thorough analysis is presented for the dependence of the efficiency of revealing common (correlated) fragments on the number of SHs and on the information characteristics of images determined, additionally, by the properties of volume HRMs and recording conditions. Results of numerical experiments are presented, which confirm theoretical conclusions. Terms and notations suggested previously in [16] are used in the present work. The term ‘image’ is a synonym of ‘pattern’ and ‘field of complex amplitudes’. The term ‘sequence’ means a partial correlation of constituting images, which are at least neighbouring. The problem statement in terms of correlation is important for juxtaposing the considered method and the more general problem of inductive generalisation [18], since it assumes that there are no *a priori* criteria, except for the occurrence frequency, for ascribing an image fragment to common for the entire sequence (or its part) or distinct (individual) fragments. Such a problem statement complicates the task because it excludes from consideration the induction methods based on the difference in other characteristics of fragments.

A.V. Pavlov ITMO University, Kronverkskii prosp. 49, 197101 St. Petersburg, Russia; e-mail: pavlov@phoi.ifmo.ru

Received 7 February 2017
Kvantovaya Elektronika **47** (4) 335–342 (2017)
Translated by N.A. Raspopov

2. Optical scheme and model

Below we describe an optical scheme and briefly remind the main results of [16] used in the present work, specifying and complementing those if needed. A 4*f* Fourier holography scheme is considered with SH recording by the joint-transform method, see Fig. 1. To simplify expressions, whenever possible, we will consider images and, correspondingly, holograms as functions of a single variable.

In the scheme shown in Fig. 1, a multiplex Fourier hologram is recorded,

$$H(v_x) = \sum_{k=1}^{n} H_k(v_x), \tag{1}$$

produced (under the assumption of recording within a linear part of the dynamic range of the HRM exposure characteristic) by imposing n pairs of SH images $S_k(x) \leftrightarrow R_k(x)$, where

$$H_k(v_x) = F(S_k(x))F^*(R_k(x))\exp[-\mathrm{j}\omega(x_k^{(R)} + x_k^{(S)})]; \tag{2}$$

F is the symbol of the Fourier transform; v_x is the spatial frequency; $\omega_x = 2\pi v_x$ is the circular spatial frequency; $x_k^{(R)}$ and $x_k^{(S)}$ are the coordinates describing the spatial position of the corresponding images relative to the principal optical axis in the entry plane; and j is an imaginary unit. We will assume that $S_k(x)$ is a signal image and $R_k(x)$ is a reference image; their sequences we denote by $\{S_k\}_{k=1}^n$ and $\{R_k\}_{k=1}^n$, respectively. The images can be presented as a sum of their fragments: common, that is, correlated (with the upper index 'c') and distinct, which play the role of background (with the upper index 'u'):

$$\begin{aligned} &S_k(x) = S_k^{\mathrm{c}}(x) + S_k^{\mathrm{u}}(x), \quad R_k(x) = R_k^{\mathrm{c}}(x) + R_k^{\mathrm{u}}(x), \\ &S_k^{\mathrm{c}}(x) = m^{(S)}S_k(x), \quad S_k^{\mathrm{u}}(x) = (1 - m^{(S)})S_k(x), \\ &R_k^{\mathrm{c}}(x) = m^{(R)}R_k(x), \quad R_k^{\mathrm{u}}(x) = (1 - m^{(R)})R_k(x), \end{aligned} \tag{3}$$

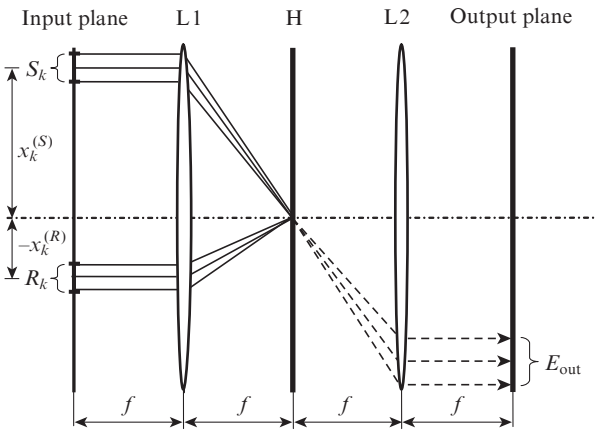

Figure 1. 4*f*-scheme of Fourier holography:
R_k, S_k are a pair of images recorded to one hologram H; $x_k^{(R)}$, $x_k^{(S)}$ are their coordinates relative to the principal optical axis; L1, L2 are the first and second Fourier-transform lenses with a focal length f; dashed lines show the beams reconstructing the field E_{out} in the output plane when the image R_k is supplied in the input plane.

where $m^{(S)}$, $m^{(R)}$ are the specific weights of correlated fragments in the corresponding images. Condition (3) admits both the spatial superposition of images and side by side placement, including the case where one fragment flows over the other. We will use the latter variant as adequate to some practical applications, for example, to analysis of a video data stream [14].

If the distinct fragments of images are orthogonal, then $m^{(S)} = \sqrt{\rho_{kl}^{(S)}}$ и $m^{(R)} = \sqrt{\rho_{kl}^{(R)}}$, where $\rho_{kl}^{(S)}$ and $\rho_{kl}^{(R)}$ are the correlation coefficients for the corresponding images in the sequences $\{S_k\}_{k=1}^n$ and $\{R_k\}_{k=1}^n$. Then, (3) can be presented in the form

$$\begin{aligned} &S_k^{\mathrm{c}}(x) = \sqrt{\rho_{kl}^{(S)}}\,S_k(x), \;\; S_k^{\mathrm{u}}(x) = \left(1 - \sqrt{\rho_{kl}^{(S)}}\right)S_k(x), \\ &R_k^{\mathrm{c}}(x) = \sqrt{\rho_{kl}^{(R)}}\,R_k(x), \;\; R_k^{\mathrm{u}}(x) = \left(1 - \sqrt{\rho_{kl}^{(R)}}\right)R_k(x). \end{aligned}$$

If the differing fragments of an image are not orthogonal then, when they are presented as realisations of a single random field, the cross correlation coefficient ρ of two realisations (under the assumption of the ergodic hypothesis – disjoint fragments) the fields and specific weights m are related by the expression:

$$\rho_{kl} = m^2(1-\rho) + \rho, \;\; m = \sqrt{\frac{\rho_{kl} - \rho}{1 - \rho}}, \tag{4}$$

where the upper indices at ρ, m and ρ_{kl} are omitted.

In was shown [16] that for solving the problem, the condition of a constant distance between the signal and reference images should be fulfilled while recording all HSs:

$$\forall_{k,l} \in [0,n]: x_k^{(R)} - x_l^{(R)} = x_k^{(S)} - x_l^{(S)}.$$

As applied to volume holograms, this condition reduces to the condition of a constant position in the entry plane for all images of processed sequences $\{S_k\}_{k=1}^n$ and $\{R_k\}_{k=1}^n$. Then, when the kth image $R_k(x)$ is presented to a multiplex hologram (1) recorded in the input plane, in the rear focal plane of the second Fourier-transform lens L2 one obtains the field of complex amplitudes (while choosing signs, we take into account the coordinate inversion related to the fact that the inverse Fourier transform cannot be realised with lenses)

$$\begin{aligned} E_{\mathrm{out}}(x) &= F(F(R_k(x))H(v_x)) \\ &= S_k(x + x_k^{(S)}) * [R_k(x) \otimes R_k(x)] \\ &+ \sum_{k \neq l} S_l(x + x_k^{(S)}) * [R_k(x) \otimes R_l(x)] = \\ &= S_k^{\mathrm{c}}(x + x_k^{(S)}) * [R_k(x) \otimes R_k(x)] \\ &+ S_k^{\mathrm{u}}(x + x_k^{(S)}) * [R_k(x) \otimes R_k(x)] \\ &+ \sum_{k \neq l} S_l(x + x_k^{(S)}) * [(R_k^{\mathrm{c}}(x) + R_k^{\mathrm{u}}(x)) \otimes (R_l^{\mathrm{c}}(x) + R_l^{\mathrm{u}}(x))] \\ &= S_k^{\mathrm{c}}(x + x_k^{(S)}) * [R_k(x) \otimes R_k(x)] \\ &+ S_k^{\mathrm{u}}(x + x_k^{(S)}) * [R_k(x) \otimes R_k(x)] \\ &+ (m^{(R)})^2(n-1)\{S_k^{\mathrm{c}}(x + x_k^{(S)}) * [R_k(x) \otimes R_k(x)]\} \\ &+ (m^{(R)})^2 \sum_{k \neq l} S_l^{\mathrm{u}}(x + x_k^{(S)}) * [R_k(x) \otimes R_k(x)] \end{aligned}$$

$$+\sum_{k\neq l} S_l(x+x_k^{(S)})*[R_k^{\mathrm{u}}(x)\otimes R_l^{\mathrm{u}}(x)]$$

$$+\sum_{k\neq l} S_l(x+x_k^{(S)})*[R_k^{\mathrm{c}}(x)\otimes R_l^{\mathrm{u}}(x)]$$

$$+\sum_{k\neq l} S_l(x+x_k^{(S)})*[R_k^{\mathrm{u}}(x)\otimes R_l^{\mathrm{c}}(x)]$$

$$=[1+(m^{(R)})^2(n-1)]\{S_k^{\mathrm{c}}(x+x_k^{(S)})*[R_k(x)\otimes R_k(x)]\}$$

$$+S_k^{\mathrm{u}}(x+x_k^{(S)})*[R_k(x)\otimes R_k(x)]$$

$$+(m^{(R)})^2\sum_{k\neq l} S_l^{\mathrm{u}}(x+x_k^{(S)})*[R_k(x)\otimes R_k(x)]$$

$$+\sum_{k\neq l} S_l(x+x_k^{(S)})*[R_k^{\mathrm{u}}(x)\otimes R_l^{\mathrm{u}}(x)]$$

$$+\sum_{k\neq l} S_l(x+x_k^{(S)})*[R_k^{\mathrm{c}}(x)\otimes R_l^{\mathrm{u}}(x)]$$

$$+\sum_{k\neq l} S_l(x+x_k^{(S)})*[R_k^{\mathrm{u}}(x)\otimes R_l^{\mathrm{c}}(x)], \qquad (5)$$

where $*$ and $\otimes$ are the symbols of convolution and correlation operations, respectively; terms in brackets in the final expression, which describe auto- and cross-correlation functions of the reference images and fragments, have the sense of the pulse responses describing the point diffraction spreading for the corresponding terms. Note that in (5), as compared to (12) from [16], all the cross-correlation terms, which are partially omitted in [16], are taken into account.

Before passing to further analysis, recall that the first summand in the final expression (5) describes the field $E_{\mathrm{out}}^{\mathrm{c}}(x)$ needed for solving the problem. This field is the common (completely correlated) fragment of signal images $\{S_k\}_{k=1}^n$, reconstructed by multiplex hologram (1). The second summand in (5) plays the role of constant noise independent of the number of SHs. It was shown [16] that in the case of the total correlation of reference images, the third summand, dependent on the number of SHs, reduces the effect of this constant noise and, thus, helps revealing the correlated fragment.

The mechanism of such revealing is based on the property of dispersion of the sum of random processes (fields) [19, 20], and the dispersion itself is used as an integral estimate of image modulation (contrast). We are interested in estimating the efficiency of revealing a correlated fragment $E_{\mathrm{out}}^{\mathrm{c}}(x)$ on the background of the field playing the role of noise, which we designate as $E_{\mathrm{out}}^{\mathrm{u}}(x)$. Such an estimate can be made in terms of the ratio of their dispersions $D_{\mathrm{out}}^{\mathrm{c}}$ and $D_{\mathrm{out}}^{\mathrm{u}}$: the growing ratio with increasing n means that the modulation of the field $E_{\mathrm{out}}^{\mathrm{u}}(x)$ reduces as compared to that of the field $E_{\mathrm{out}}^{\mathrm{c}}(x)$. In other words, the noticeably modulated $E_{\mathrm{out}}^{\mathrm{c}}(x)$ is well distinguished on the background of $E_{\mathrm{out}}^{\mathrm{u}}(x)$ that becomes more and more homogeneous (grey) as n increases. As a first approximation, only the first three summands (5) were taken into account in [16]. Below we will perform an analysis taking into account all the summands and arbitrary values of the cross-correlation factor for distinct fragments of the reference images. This requires taking into account both the properties of hologram (1) from the viewpoint of conservation or nonconservation of the Fourier transform invariance with respect to shift, and the information characteristics of images.

3. Estimate of the efficiency of revealing correlated fragments

3.1. Influence of hologram three-dimensionality

Each of the summands included in the description of the reconstructed field (5) is a convolution with the terms in brackets that have the sense of pulsed responses: autocorrelation functions (ACFs) of the reference images $[R_k(x)\otimes R_k(x)]$ (for the first three summands) and their distinct fragments $[R_k^{\mathrm{u}}(x)\otimes R_l^{\mathrm{u}}(x)]$ (for the fourth summand), or joint correlation functions (JCFs) $[R_k^{\mathrm{c}}(x)\otimes R_l^{\mathrm{u}}(x)]$ of their fragments (for the fifth and sixth summands). The contribution of the field components $E_{\mathrm{out}}^{\mathrm{c}}(x)$ and $E_{\mathrm{out}}^{\mathrm{u}}(x)$ (5) is directly affected by the appearance of the terms in brackets included in the fourth, fifth, and sixth summands in (5), namely, by the possibility of presenting them via unimodal (having a single maximum) or by only multimodal (having several maxima of comparable values) functions. Competence or, inversely, incompetence of such presentation is determined, in turn, by the conservation or nonconservation of the Fourier transform invariance with respect to the shift in the scheme from Fig. 1 while using volume or thin HRMs, respectively:

– if the shift invariance is not preserved (volume hologram), then the terms in brackets are unimodal functions and one should take into account only the value corresponding to the origin of coordinates in the correlation space;

– if the shift invariance is preserved (thin holograms), then the terms in brackets as JCFs are multimodal functions and all the correlation maxima should be taken into account – as the global one corresponding to the origin of coordinates in the correlation space, so and side maxima.

Since the maximal storage density of holographic memory is attained by using volume HRMs [5–7], we consider this case.

3.2. Estimation of the revealing efficiency for a volume hologram

If we deal with a volume HRM then, due to the nonconservation of the Fourier transform invariance with respect to the shift, both the auto- and cross-correlation terms in brackets included in expression (5) can be approximated by unimodal (with a single maximum) functions. In this case, for JCFs the only maximum is important for which the coordinate in the correlation space coincides with the coordinate of the ACF global maximum, that is, the maximum corresponding to a zero shift. Then, by expanding the signal images included in the fourth-sixth summands (5) into the sum of common (totally correlated) and distinct fragments according to (3), the reconstructed field (5) can be presented as the sum of the two fields:
the field of common fragments

$$E_{\mathrm{out}}^{\mathrm{c}}(x)=[1+(m^{(R)})^2(n-1)]$$

$$\times\{S_k^{\mathrm{c}}(x+x_k^{(S)})*[R_k(x)\otimes R_k(x)]\}$$

$$+\sum_{k\neq l} S_l^{\mathrm{c}}(x+x_k^{(S)})*[R_k^{\mathrm{u}}(x)\oplus R_l^{\mathrm{u}}(x)]$$

$$+\sum_{k\neq l} S_l^{\mathrm{c}}(x+x_k^{(S)})*[R_k^{\mathrm{c}}(x)\oplus R_l^{\mathrm{u}}(x)]$$
$$+\sum_{k\neq l} S_l^{\mathrm{c}}(x+x_k^{(S)})*[R_k^{\mathrm{u}}(x)\oplus R_l^{\mathrm{c}}(x)]$$
$$=[1+(m^{(R)})^2(n-1)]\{S_k^{\mathrm{c}}(x+x_k^{(S)})*[R_k(x)\otimes R_k(x)]\}$$
$$+(n-1)S_k^{\mathrm{c}}(x+x_k^{(S)})*[R_k^{\mathrm{u}}(x)\otimes R_l^{\mathrm{u}}(x)]$$
$$+(n-1)S_k^{\mathrm{c}}(x+x_k^{(S)})*[R_k^{\mathrm{c}}(x)\otimes R_l^{\mathrm{u}}(x)]$$
$$+(n-1)S_k^{\mathrm{c}}(x+x_k^{(S)})*[R_k^{\mathrm{u}}(x)\otimes R_l^{\mathrm{c}}(x)] \qquad (6)$$

and the field of distinct (partially correlated) fragments

$$E_{\mathrm{out}}^{\mathrm{u}}(x)=S_k^{\mathrm{u}}(x+x_k^{(S)})*[R_k(x)\otimes R_k(x)]$$
$$+(m^{(R)})^2\sum_{k\neq l} S_l^{\mathrm{u}}(x+x_k^{(S)})*[R_k(x)\otimes R_k(x)]$$
$$+\sum_{k\neq l} S_l^{\mathrm{u}}(x+x_k^{(S)})*[R_k^{\mathrm{u}}(x)\otimes R_l^{\mathrm{u}}(x)]$$
$$+\sum_{k\neq l} S_l^{\mathrm{u}}(x+x_k^{(S)})*[R_k^{\mathrm{c}}(x)\otimes R_l^{\mathrm{u}}(x)]$$
$$+\sum_{k\neq l} S_l^{\mathrm{u}}(x+x_k^{(S)})*[R_k^{\mathrm{u}}(x)\otimes R_l^{\mathrm{c}}(x)]. \qquad (7)$$

Consider the field of common fragments $E_{\mathrm{out}}^{\mathrm{c}}(x)$(6). The global maximum amplitude of ACFs for the reference images $[R_k(x)\otimes R_k(x)]$ can be estimated [19, 21] as

$$\mu^{\mathrm{ACF}}=\max[R_k(x)\otimes R_k(x)]=D_{k\mathrm{out}}^{(R)}L_x^{(R)}L_y^{(R)}, \qquad (8)$$

where $D_{k\mathrm{out}}^{(R)}$ is the dispersion of the reference image reconstructed with the nonlinearity of the hologram exposure characteristic of HRM filtration on the hologram taken into account; and $L_x^{(R)}$, $L_y^{(R)}$ are the reference image dimensions assuming a rectangular shape of the frame window.

In the case of JCFs for distinct fragments of reference images $[R_k^{\mathrm{u}}(x)\otimes R_l^{\mathrm{u}}(x)]$, we, due to the nonconservation of the shift invariance by volume holograms, are interested in the amplitude of only one maximum, whose average value can be estimated by the formula

$$\mu^{\mathrm{CCF}}=\langle[R_k^{\mathrm{u}}(x)\otimes R_l^{\mathrm{u}}(x)]\rangle\approx D_{k\mathrm{out}}^{(R)}r_{k\mathrm{out}}\sqrt{L_x^{(R)\mathrm{u}}L_y^{(R)\mathrm{u}}2\pi\kappa}$$
$$=D_{k\mathrm{out}}^{(R)}\sqrt{L_x^{(R)\mathrm{u}}L_y^{(R)\mathrm{u}}2\pi r_{k\mathrm{out}}^2\kappa}=$$
$$=D_{k\mathrm{out}}^{(R)}L_x^{(R)\mathrm{u}}L_y^{(R)\mathrm{u}}\sqrt{2\frac{\pi r_{k\mathrm{out}}^2}{L_x^{(R)\mathrm{u}}L_y^{(R)\mathrm{u}}}\kappa}$$
$$=D_{k\mathrm{out}}^{(R)}L_x^{(R)\mathrm{u}}L_y^{(R)\mathrm{u}}\sqrt{\frac{2\kappa}{\Omega^{(R)\mathrm{u}}}},$$

where angular brackets denote averaging over the ensemble; $r_{k\mathrm{out}}$ is the correlation radius of the reconstructed field; k is the coefficient dependent on the correlation function shape; $\Omega^{(R)\mathrm{u}}=L_x^{(R)\mathrm{u}}L_y^{(R)\mathrm{u}}/(\pi r_{\mathrm{out}}^2)$ is the correlation estimate of the information capacity for distinct fragments. For an exponential correlation function at not very small estimates of information capacity, we can take $\kappa\approx 0.25$ [21]. Since, according to (3), $L_x^{(R)\mathrm{u}}L_y^{(R)\mathrm{u}}=(1-m^{(R)})L_x^{(R)\mathrm{u}}L_y^{(R)\mathrm{u}}$ we have $\Omega^{(R)\mathrm{u}}=(1-m^{(R)})\Omega^{(R)}$ ($\Omega^{(R)}$ is the estimate for the information capacity). The final expression for the average amplitude of the term under the sum sign in the third summand (6) can be presented in the form convenient for further comparison:

$$\mu^{\mathrm{CCF}}\approx D_{k\mathrm{out}}^{(R)}L_x^{(R)\mathrm{u}}L_y^{(R)\mathrm{u}}\sqrt{\frac{2\kappa}{\Omega^{(R)\mathrm{u}}}}$$
$$=D_{k\mathrm{out}}^{(R)}L_x^{(R)\mathrm{u}}L_y^{(R)\mathrm{u}}\sqrt{(1-m^{(R)})\frac{2\kappa}{\Omega^{(R)}}}$$
$$=\mu^{\mathrm{ACF}}\sqrt{(1-m^{(R)})\frac{2\kappa}{\Omega^{(R)}}}. \qquad (9)$$

The estimate of the contribution from the third and fourth summands in (6) depends on mutual disposition of common and distinct fragments in the reference images. If they are superimposed, then the correlation maximum should be taken into account, which amplitude is determined by the dimension of the smallest fragment of the reference images $R_l^{\mathrm{c}}(x)$ and $R_k^{\mathrm{u}}(x)$. For this purpose, let us introduce the ratio of their dimensions t taking into account (3) in the following way:

$$t=m^{(R)}\ \text{ if }\ m^{(R)}\leqslant 0.5,$$
$$t=1-m^{(R)}\ \text{ if }\ m^{(R)}\geqslant 0.5. \qquad (10)$$

Then, by analogy with derivation of expression (9) and in view of (10) we have

$$\mu^{\mathrm{CCF}}=\langle[R_k^{\mathrm{c}}(x)\otimes R_l^{\mathrm{u}}(x)]\rangle\approx$$
$$\approx D_{k\mathrm{out}}^{(R)}L_x^{(R)\mathrm{u}}L_y^{(R)\mathrm{u}}\sqrt{t\frac{2\kappa}{\Omega^{(R)}}}=\mu^{\mathrm{ACF}}\sqrt{t\frac{2\kappa}{\Omega^{(R)}}}. \qquad (11)$$

Taking into account (11) we obtain the expression for upper estimate of the reconstructed field of common fragment:

$$E_{\mathrm{out}}^{\mathrm{c}}(x)=[1+(m^{(R)})^2(n-1)]$$
$$\times\{S_k^{\mathrm{c}}(x+x_k^{(S)})*[R_k(x)\otimes R_k(x)]\}$$
$$+(n-1)\sqrt{(1-m^{(R)})\frac{2\kappa}{\Omega^{(R)}}}$$
$$\times S_k^{\mathrm{c}}(x+x_k^{(S)})*[R_k(x)\otimes R_k(x)]$$
$$+(n-1)2\sqrt{t\frac{2\kappa}{\Omega^{(R)}}}S_k^{\mathrm{c}}(x+x_k^{(S)})*[R_k(x)\otimes R_k(x)]=$$
$$=[1+(n-1)K(m^{(R)})]$$
$$\times\{S_k^{\mathrm{c}}(x+x_k^{(S)})*[R_k(x)\otimes R_k(x)]\}, \qquad (12)$$

where

$$K(m^{(R)})=\left[(m^{(R)})^2+\sqrt{(1-m^{(R)})\frac{2\kappa}{\Omega^{(R)}}}+2\sqrt{t\frac{2\kappa}{\Omega^{(R)}}}\right]$$

is the term dependent on the information characteristics of the reference image sequence and on the specific weight $m^{(R)}$ of the common fragment in the reference image.

If the common and distinct fragments of reference images are not superimposed, then the maximum of the JCF should be taken into account, which is in a falling part of the latter. In this case, for obtaining the lower estimate one should simply neglect the corresponding term (11) in expression (12).

Dispersion of the reconstructed field of the common fragment is

$$D_{\Sigma}^{\mathrm{c}} = [1 + (n-1)K(m^{(R)})]^2 D_{k\mathrm{out}}^{(S)\mathrm{c}}, \tag{13}$$

where $D_{k\mathrm{out}}^{(S)\mathrm{c}}$ is the dispersion of the reconstructed image of one SH in the common fragment. In view of (4) one can see that at the total correlation of the reference images ($\rho_{kl}^{(R)} = 1$) it coincides with an approximate estimate given in [16].

Consider the field of distinct fragments $E_{\mathrm{out}}^{\mathrm{u}}(x)$ (7). Since the summation order for all summands in (7), except for the first, is the same, it suffices to estimate the specific weights for the terms under the summation sign. The specific weight of the second-fifth summands in (7) is determined by the corresponding terms in brackets; hence, one can employ the analysis of expressions (8)–(11) performed above. By using results of the analysis, one may present (7) in the form

$$\begin{aligned} E_{\mathrm{out}}^{\mathrm{u}}(x) &= S_k^{\mathrm{u}}(x + x_k^{(S)}) * [R_k(x) \otimes R_k(x)] \\ &+ (m^{(R)})^2 \sum_{k \neq l} S_l^{\mathrm{u}}(x + x_k^{(S)}) * [R_k(x) \otimes R_k(x)] \\ &+ \sqrt{(1 - m^{(R)})\frac{2\kappa}{\Omega^{(R)}}} \\ &\times \sum_{k \neq l} S_l^{\mathrm{u}}(x + x_k^{(S)}) * [R_k(x) \otimes R_k(x)] \\ &+ 2\sqrt{t\frac{2\kappa}{\Omega^{(R)}}} \sum_{k \neq l} S_l^{\mathrm{u}}(x + x_k^{(S)}) * [R_k(x) \otimes R_k(x)] \\ &= S_k^{\mathrm{u}}(x + x_k^{(S)}) * [R_k(x) \otimes R_k(x)] \\ &+ K(m^{(R)}) \sum_{k \neq l} S_l^{\mathrm{u}}(x + x_k^{(S)}) * [R_k(x) \otimes R_k(x)]. \end{aligned} \tag{14}$$

From this, the dispersion of the field-noise $E_{\mathrm{out}}^{\mathrm{u}}(x)$can be presented in the form

$$\begin{aligned} D_{\Sigma}^{\mathrm{u}} &= D\Bigg(S_k^{\mathrm{u}}(x + x_k^{(S)}) * [R_k(x) \otimes R_k(x)] + K(m^{(R)}) \\ &\times \sum_{k \neq l} S_l^{\mathrm{u}}(x + x_k^{(S)}) * [R_k(x) \otimes R_k(x)] \Bigg) = D_{k\mathrm{out}}^{(S)\mathrm{u}} + K^2(m^{(R)}) \\ &\times D\Bigg(\sum_{k \neq l} S_l^{\mathrm{u}}(x + x_k^{(S)}) * [R_k(x) \otimes R_k(x)] \Bigg) + 2D_{12}, \end{aligned} \tag{15}$$

where $D(...)$ is the dispersion; $D_{k\mathrm{out}}^{(S)\mathrm{u}}$ is the dispersion of the first summand; and D_{12} are the covariances of the summands in the upper line (15).

The second summand in the final expression (15) can be presented, with the neglected multiplier $K^2(m^{(R)})$, in the form

$$\begin{aligned} &D\Bigg(\sum_{k \neq l} S_l^{\mathrm{u}}(x + x_k^{(S)}) * [R_k(x) \otimes R_k(x)] \Bigg) \\ &= \{(1-n) D(S_l^{\mathrm{u}}(x + x_k^{(S)}) * [R_k(x) \otimes R_k(x)]) \\ &+ (n-1)(n-2) D_{kl\mathrm{out}}^{(S)\mathrm{u}}\} = (n-1) D_{k\mathrm{out}}^{(S)\mathrm{u}} \left[1 + (n-2)\frac{D_{kl\mathrm{out}}^{(S)\mathrm{u}}}{D_{k\mathrm{out}}^{(S)\mathrm{u}}} \right] \\ &= (n-1) D_{k\mathrm{out}}^{(S)\mathrm{u}} \left[1 + (n-2)\sqrt{\frac{2\kappa}{\Omega^{(S)\mathrm{u}}}} \right], \end{aligned} \tag{16}$$

where $D_{kl\mathrm{out}}^{(S)\mathrm{u}}$ is the covariance of the reconstructed distinct fragments in signal images; and $\Omega^{(S)\mathrm{u}}$ is the correlation estimate for the information capacity of fragments.

Covariance D_{12}, by using the definition of the correlation factor $\rho_{xy} = D_{xy}/(\sigma_x \sigma_y)$, where σ_x and σ_y are the root-mean-square deviations [19], can be presented in the form

$$\begin{aligned} D_{12} &= \rho_{kl\mathrm{out}}^{(S)\mathrm{u}} K(m^{(R)}) \\ &\times \Bigg\{ D(S_k^{\mathrm{u}}(x + x_k^{(S)}) * [R_k(x) \otimes R_k(x)]) \\ &\times D\Bigg(\sum_{k \neq l} S_l^{\mathrm{u}}(x + x_k^{(S)}) * [R_k(x) \otimes R_k(x)] \Bigg) \Bigg\}^{1/2} \\ &= D_{k\mathrm{out}}^{(S)\mathrm{u}} \rho_{kl\mathrm{out}}^{(S)\mathrm{u}} K(m^{(R)}) \sqrt{(n-1)\left[1 + (n-2)\sqrt{\frac{2\kappa}{\Omega^{(S)\mathrm{u}}}} \right]}, \end{aligned} \tag{17}$$

where $\rho_{kl\mathrm{out}}^{(S)\mathrm{u}}$ is the correlation factor for distinct fragments with the filtering on a hologram taken into account. According to [21], we have $\rho_{kl\mathrm{out}}^{(S)\mathrm{u}} = (2\kappa/\Omega^{(S)\mathrm{u}})^{1/2}$, and the dispersion of the noise-field is

$$\begin{aligned} D_{\Sigma}^{\mathrm{u}} &= D_{k\mathrm{out}}^{(S)\mathrm{u}} \Bigg\{ 1 + K^2(m^{(R)})(n-1)\left[1 + (n-2)\sqrt{\frac{2\kappa}{\Omega^{(S)\mathrm{u}}}} \right] \\ &+ 2K(m^{(R)})\sqrt{\frac{2\kappa}{\Omega^{(S)\mathrm{u}}}} \sqrt{(n-1)\left[1 + (n-2)\sqrt{\frac{2\kappa}{\Omega^{(S)\mathrm{u}}}} \right]} \Bigg\}. \end{aligned} \tag{18}$$

Now we obtain the estimate for the efficiency of revealing common fragments on the background of distinct fragments in terms of the ratio of their dispersions

$$\begin{aligned} V_n &= \frac{D_{\Sigma}^{\mathrm{c}}}{D_{\Sigma}^{\mathrm{u}}} = \frac{D_{k\mathrm{out}}^{(S)\mathrm{c}}}{D_{k\mathrm{out}}^{(S)\mathrm{u}}} [1 + (n-1)K(m^{(R)})]^2 \\ &\times \Bigg\{ 1 + K^2(m^{(R)})(n-1)\left[1 + (n-2)\sqrt{\frac{2\kappa}{\Omega^{(S)\mathrm{u}}}} \right] \\ &+ 2K(m^{(R)})\sqrt{\frac{2\kappa}{\Omega^{(S)\mathrm{u}}}} \sqrt{(n-1)\left[1 + (n-2)\sqrt{\frac{2\kappa}{\Omega^{(S)\mathrm{u}}}} \right]} \Bigg\}^{-1}. \end{aligned} \tag{19}$$

3.3. Analysis and discussion

Since we assume that all the images are realisations of the same homogeneous random field, we have $D_{k\mathrm{out}}^{(S)\mathrm{c}} = D_{k\mathrm{out}}^{(S)\mathrm{u}}$. In further consideration, it is convenient to represent (19) in the form

$$\begin{aligned} V(n) &= \frac{D_{\Sigma}^{\mathrm{c}}}{D_{\Sigma}^{\mathrm{u}}} \propto [1 + (n-1)K(m^{(R)})]^2 \\ &\times \Bigg\{ \Bigg\{ 1 + K(m^{(R)})\sqrt{(n-1)\left[1 + (n-2)\sqrt{\frac{2\kappa}{\Omega^{(S)\mathrm{u}}}} \right]} \Bigg\}^2 \\ &- 2K(m^{(R)})\left(1 - \sqrt{\frac{2\kappa}{\Omega^{(S)\mathrm{u}}}} \right) \\ &\times \sqrt{(n-1)\left[1 + (n-2)\sqrt{\frac{2\kappa}{\Omega^{(S)\mathrm{u}}}} \right]} \Bigg\}^{-1}. \end{aligned} \tag{20}$$

From analysis of (20) one may draw the following conclusions:

1. With a growth of the SH number n, the estimate saturates; the saturation level is determined by the information characteristics of signal images, namely, by the correlation estimate of the information capacities of their fragments

$\Omega^{(S)u}$ and the parameter k, which depends on the shape of the ACF field [21]. Omitting cumbersome formulae, for practical use one can employ the approximate estimate of the saturation level:

$$\lim_{n\to\infty} V(n) \approx \sqrt{\frac{\Omega^{(S)u}}{2\kappa}} \approx (\rho^{(S)u}_{kl\text{out}})^{-1}. \quad (21)$$

The dependence of the saturation level (21) only on the information estimate of distinct fragments of signal images $\Omega^{(S)u}$ relates to the mechanism of revealing common fragments by background smoothing: with a growth of the SH number n, only the normalised estimates of the dispersion for distinct fragments vary, whereas the normalised dispersion of common fragments is independent of n.

From the practical point of view, this effect determined in the context of the inductive generalisation problem as the phenomenon of cognitive saturation [22] implies the existence of a certain effective SH number n_{eff}, determined by reaching a prescribed threshold for the first derivative (19) with respect to n. Above the threshold, there is no further noticeable increase in the estimate of the revealing efficiency for correlated fragments with an increase in the number of SHs.

In turn, the estimate of the information capacity for distinct fragments of signal images $\Omega^{(S)u}$ depends on the HRM properties and conditions of hologram recording: a limited dynamic range of the HRM results in a narrowed frequency band, which, according to the Wiener–Khintchine theorem, leads to a change in the correlation radius included in the expression for $\Omega^{(S)u}$. A thorough analysis of this relationship is beyond the scope of the present consideration and warrants separate investigation.

2. The characteristics of the reference images, such as the correlation factor $\rho^{(R)}_{kl}$ and the estimate of the information capacity $\Omega^{(R)}$, comprised in the expression for term $K(m^{(R)})$ play a noticeable role mainly in the range of small n at large values of $\Omega^{(R)}$ and affect the rate of reaching saturation (21), but not the saturation level itself.

3. If the distinct fragments of signal images are orthogonal, then by definition $D^{(S)u}_{kl\text{out}} = 0$ and in view of (16) and (17) we have $(2\kappa/\Omega^{(S)u})^{1/2} \equiv 0$, and (19) takes the form

$$V(n) = \frac{D^{c}_{\Sigma}}{D^{u}_{\Sigma}} = \frac{D^{(S)c}_{k\text{out}}}{D^{(S)u}_{k\text{out}}} \frac{[1+(n-1)K(m^{(R)})]^2}{[1+(n-1)K^2(m^{(R)})]}. \quad (22)$$

In the first approximation for not small n, expression (22) can be approximated by a linear function.

If the reference images are totally correlated, then $K(m^{(R)}) = 1$ and we obtain the linear dependence:

$$V(n) = \frac{D^{c}_{\Sigma}}{D^{u}_{\Sigma}} = n\frac{D^{(S)c}_{k\text{out}}}{D^{(S)u}_{k\text{out}}}, \quad (23)$$

which coincides with results presented in [15, 16].

4. Expressions (19) and (20) are sufficiently cumbersome; hence, it is worth finding a simpler approximation expression suitable for practical use. From this point of view, the approximating formula should provide acceptable estimates for the saturation level, that is, for the effective number of SHs n_{eff}. Then for not small estimates of the information capacity of distinct fragments of reference images $\Omega^{(R)u}$ one can take $K(m^{(R)}) \approx (m^{(R)})^2$ which entails

$$V(n) = \frac{D^{c}_{\Sigma}}{D^{u}_{\Sigma}} \approx \frac{D^{(S)c}_{k\text{out}}}{D^{(S)u}_{k\text{out}}}[1+(n-1)(m^{(R)})^2]^2 \times\left\{1+(m^{(R)})^4(n-1)\left[1+(n-2)\sqrt{\frac{2\kappa}{\Omega^{(S)u}}}\right] + 2(m^{(R)})^2\sqrt{\frac{2\kappa}{\Omega^{(S)u}}}\sqrt{(n-1)\left[1+(n-2)\sqrt{\frac{2\kappa}{\Omega^{(S)u}}}\right]}\right\}^{-1}.$$

In practice, the common fragment does not dominate in the signal image, that is, $(2\kappa/\Omega^{(S)u})^{1/2} \ll 1$ and one can neglect the third summand in the denominator of this formula to obtain the approximating expression

$$V(n) \approx \frac{D^{(S)c}_{k\text{out}}}{D^{(S)u}_{k\text{out}}} \frac{[1+(n-1)(m^{(R)})^2]^2}{\left\{1+(m^{(R)})^4(n-1)\left[1+(n-2)\sqrt{\frac{2\kappa}{\Omega^{(S)u}}}\right]\right\}}. \quad (24)$$

Formula (24) yields, as compared to (19), a noticeable inaccuracy in the range $n < n_{\text{eff}}$; however, at $n \geqslant n_{\text{eff}}$ the estimates by (19) and (22) become comparable.

4. Numerical simulation

The theoretical conclusions were illustrated by modelling a classical variant of inductive generalisation on an example of the converse syllogism 'Darii':

Socrates is a man, Socrates is mortal;
Plato is a man, Plato is mortal;
...
All men are mortal.

The images 'Socrates Men' (reference in holography terms or index in terms of the inductive conclusion) and 'Socrates Mortal' (signal or induced, respectively) and all following images were realisations of a random field of size 256×256 pixel and comprised the two fragments:

– common realisations of the field in the form of strings 'Men' for the entire sequence of the reference images and in the form of string 'Mortal' for signal images; their specific weights (3) were $1 - m^{(R)} = 0.369$ and $1 - m^{(S)} = 0.375$, respectively;

– distinct fragments comprising individual names as well, i.e. various realisations of the field with the same statistical characteristics.

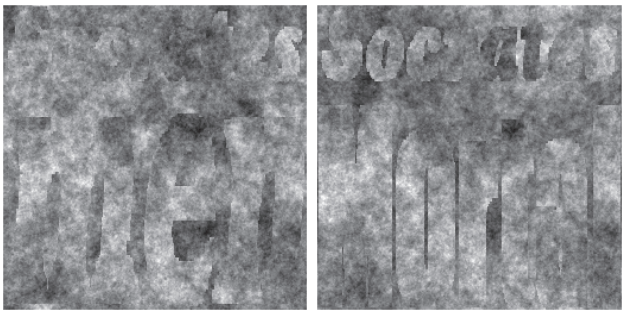

a b

Figure 2. (a) Reference image 'Socrates Men' and (b) signal image 'Socrates Mortal' in realisation of the two-dimensional fractal Brownian motion.

The first pair of images is shown in Fig. 2. These are prepared as realisations of the field described by the model of the two-dimensional fractal Brownian motion with the Hurst coefficient $H = 0.1$. Several image sequences have been prepared by the method of spatial filtering (Gaussian filter), which differed by the field correlation radius r: it varied from $r < 1$ (delta-correlated field) to $r = 10$ pixel. The estimates of the information capacity varied correspondingly, including estimate $\Omega^{(S)u}$ comprised in (19). In Fig. 3, the same images as in Fig. 2 are shown, but for the delta-correlated field. One can see that in this case, the internal correlation of images is broken and strings readable in Fig. 2 are not visually distinguished now.

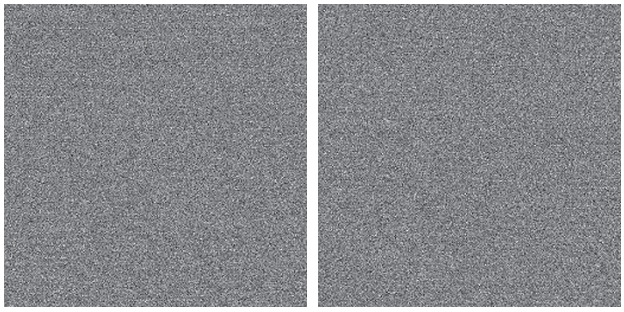

a b

Figure 3. (a) Reference image 'Socrates Men' and (b) signal image 'Socrates Mortal' in realisation of the delta-correlated field.

A record $n = 63$ SH was modelled, and the ratio of dispersions $V(n)$ for common and distinct fragments was measured in the field, reconstructed in the output plane. At this stage, an unlimited dynamic range of the HRM was assumed. Amplitudes of the reconstructed field were normalised taking into account a limited dynamic range of the sensor. Characteristics of recorded images are given in Table 1, the correlation radii correspond to blurring radii for the initial delta-correlated field of the Gaussian function.

Examples of reconstructed fields are shown in Fig. 4 at the SH number $n = 59$ for the case of delta-correlated field and at the correlation radius $r = 2$ and 10 pixel (see Table 1). In Fig. 5 one can see dependences $V(n)$ measured in a numerical experiment for various estimates of the information capacity for distinct fragments of signal images. For clarity, the theoretical estimates (19) are not presented in Fig. 5 because those well agree with the experimental values. In Fig. 6, relative

Table 1. Information characteristics of images used in the numerical experiment.

Curve number in Figs 5 and 6	Correlation radius r/pixel	Estimate of the information capacity for distinct fragments $\Omega^{(S)u}$	Estimate of the information capacity for a common fragment $\Omega^{(S)c}$	Saturation level (21)
1	< 1 (delta-correlated field)	∞	∞	∞
2	1	13050	7815	161
3	2	3260	1954	80
4	3	1450	868	54
5	4	815	488	40
6	5	521	312	32
7	7.5	232	139	21.5
8	10	130	78	16

errors of the experimental data (Fig. 4) are given as compared to the theoretical estimates (19).

From analysis of Figs 5 and 6 one may conclude:

1. The accuracy of theoretical estimate (19) increases with the SH number n. In analogue processing, the accuracy of 10% is normal; hence, the accuracy of estimate (19) at $n \geqslant 15$ for the curves (*3*–*7*) is quite satisfactory.

2. Estimate (19) fails for the images as realisations of delta-correlated fields [curves (*1*) and (*2*)]. This is explained by the fact that the internal correlation of images is totally broken and the information transfers to white noise, which is accompanied by a sharp increase in the image dispersion. The latter factor was not taken into account in deriving (19).

The method discussed efficiently reveals information hidden in noise – inscription unreadable on the etalon (Fig. 3b) image is reliably readable in the image reconstructed at $n = 59$ SHs (Fig. 4a).

3. Expression (19) also gives an unsatisfactory estimate at a very low estimate of the information capacity for the common fragment $\Omega^{(S)c}$ [curve (*8*)]. The reason is well seen in Fig. 4c: the mechanism of background smoothing $E^{u}_{out}(x)$ (7) works as efficiently as in other cases; however, the fragment to be revealed (string 'Mortal') is so spurious ($\Omega^{(S)c} = 78$) that actually cannot be read on the homogeneous background.

5. Conclusions

Thus, the scheme of Fourier holography with SHs recorded to a volume recording medium from a sequence of image pairs allows one to solve the problem of revealing common

a b c

Figure 4. Reconstructed $n = 59$ SH image for realisation of delta-correlated field (a), and with the correlation radius $r = 2$ (b) and 10 pixel (c).

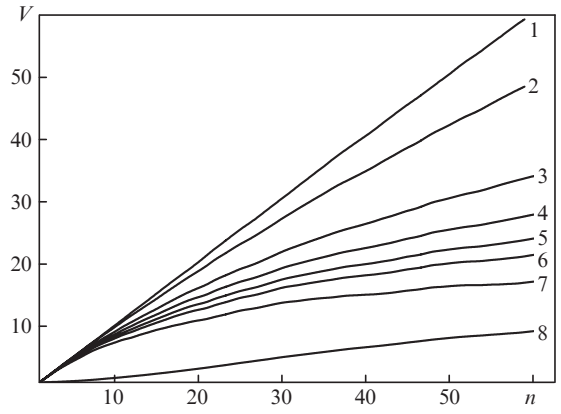

Figure 5. Dependences of the ratio of dispersions for common and distinct fragments in the reconstructed field on the SH number n at the image characteristics given in Table 1.

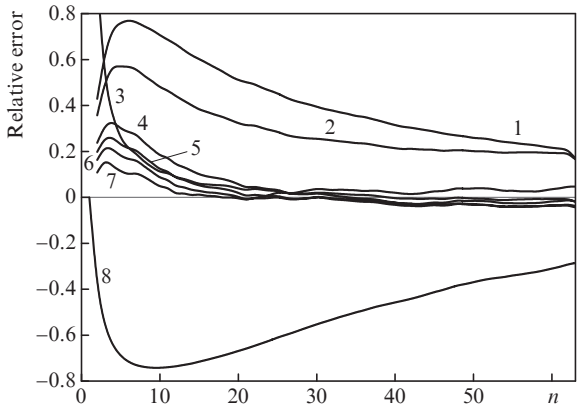

Figure 6. Relative error of experimental and theoretical (19) dependences of the ratio of dispersions of common and distinct fragments in the reconstructed field on the SH number n at the image characteristics from Table 1.

fragments of signal images. The revealing efficiency is determined by the estimate of the information capacity for distinct fragments in the signal images, except for the case of a very low estimate of the information capacity of the common fragments to be revealed. The theoretical estimate obtained yields a satisfactory accuracy as compared to experimental data at 'reasonable' values of the information characteristics of an image, first of all, at a sufficient information capacity of the common fragments themselves.

It is shown that the dependence of revealing common fragment on the number of SHs exhibits a nonlinear character attaining saturation at the level determined by the information capacity estimate for distinct fragments of signal images. This fact is related to the mechanism that provides revealing common fragments, namely, smoothing of distinct fragments as a background with a raising number of SHs. Dependence of the information characteristics of recorded images on the number of SHs is determined by a limited dynamic range of HRM. In turn, this results in a change of the saturation level. This mechanism deserves a particular investigation. The author hopes to present the corresponding results elsewhere.

Thus, new possibilities of volume Fourier SHs are shown in the frameworks of developing optical information technologies. Such possibilities are interesting for practice, in particular, in real-time analysis systems of replenished archive databases including supervisory control systems [5–7, 14]. The method suggested can be also applied for revealing hidden common fragments in delta-correlated images, which look like white noise.

Acknowledgements. The author is grateful to O.P. Kuznetsov and I.B. Fominykh for discussions and critical remarks, which favoured the formation of the approach developed.

The work was supported by the Russian Foundation for Basic Research (Grant No. 15-01-04111-a).

References

1. Van Heerden P.J. *Appl. Opt.*, **2**, 387 (1963).
2. Mikaelyan A.L., Bobrinev V.I. *Dokl. Akad. Nauk SSSR*, **191**, 799 (1970).
3. Mikaelyan A.L., Bobrinev V.I. *Radiotekhnika*, **29**, 7 (1974).
4. Lyavshuk I.A., Lyalikov A.M. *Quantum Electron.*, **36**, 154 (2006) [*Kvantovaya Elektron.*, **36**, 154 (2006)].
5. Betin A.Yu., Bobrinev V.I., Evtikhiev N.N., Zherdev A.Yu., Zlokazov E.Yu., Lushnikov D.S., Markin V.V., Odinokov S.B., Starikov S.N., Starikov R.S. *Quantum Electron.*, **43**, 87 (2013) [*Kvantovaya Elektron.*, **43**, 87 (2013)].
6. Betin A.Yu., Bobrinev V.I., Odinokov S.B., Evtikhiev N.N., Starikov R.S., Starikov S.N., Zlokazov E.Yu. *Appl. Opt.*, **52**, 8142 (2013).
7. Betin A.Yu., Bobrinev V.I., Verenikina N.M., Donchenko S.S., Evtikhiev N.N., Zlokazov E.Yu., Odinokov S.B., Starikov S.N., Starikov R.S. *Quantum Electron.*, **45**, 771 (2015) [*Kvantovaya Elektron.*, **45**, 771 (2015)].
8. Longuet-Higgins H.C. *Nature*, **217**, 104 (1968).
9. Gabor D. *Nature*, **217**, 584 (1968).
10. Mager H.J., Wess O., Waidelich W. *Opt. Commun.*, **9**, 156 (1973).
11. Borkova V.N., Zubov V.A., Kraiskii A.V. *Opt. Spectrosk.*, **63**, 384 (1987).
12. Kraiskii A.V., Mironova T.V. *Quantum Electron.*, **45**, 759 (2015) [*Kvantovaya Elektron.*, **45**, 759 (2015)].
13. Foster D.J., Wilson M.A. *Nature*, **440**, 680 (2006).
14. Garbuk S.V. *Natsional'naya Bezopasnot'*, **4**, 451 (2016).
15. Pavlov A.V. *Russ. Phys. J.*, **58** (10), 1448 (2016).
16. Pavlov A.V. *Quantum Electron.*, **46**, 759 (2016) [*Kvantovaya Elektron.*, **46**, 759 (2016)].
17. Densyuk Yu.N., Davydova I.N. *Opt. Spektrosk.*, **60**, 365 (1986).
18. Vagin V.N., Golovina E.Yu., Zagoryanskaya A.A., Fomina M.V. *Dostovernyi i pravdopodobnyi vyvod v intellektual'nykh sistemakh* (Authentic and Plausible Conclusion in Intellectual Systems) (Moscow: Fizmatlit, 2008).
19. Yaglom A.M. *Korrelyatsionnaya teoriya statsionarnykh sluchainykh funktsii* (Correlation Theory of Stationary Random Functions) (Leningrad: Gidrometeoizdat, 1981).
20. Venttsel' E.S. *Teoriya veroyatnostei: Uchebnik dlya vuzov* (Probability Theory: Textbook for High Education Institutions) (Moscow: Vysshaya shkola, 1999).
21. Shubnikov E.I. *Opt. Spektrosk.*, **62**, 450 (1987).
22. Pavlov A.V. *Trudy Pyatnadtsatoi natsional'noi konferentsii po iskusstvennomu intellektu s mezhdunarodnym uchastiem* (KII-2016) (Proceedings of the XVth National Conference on Artificial Intelligence) (Smolensk, 2016) Vol. 2, p.274.